Liposome-based vaccines for immune modulation: from antigen selection to nanoparticle design

Lozano Vigario, F.

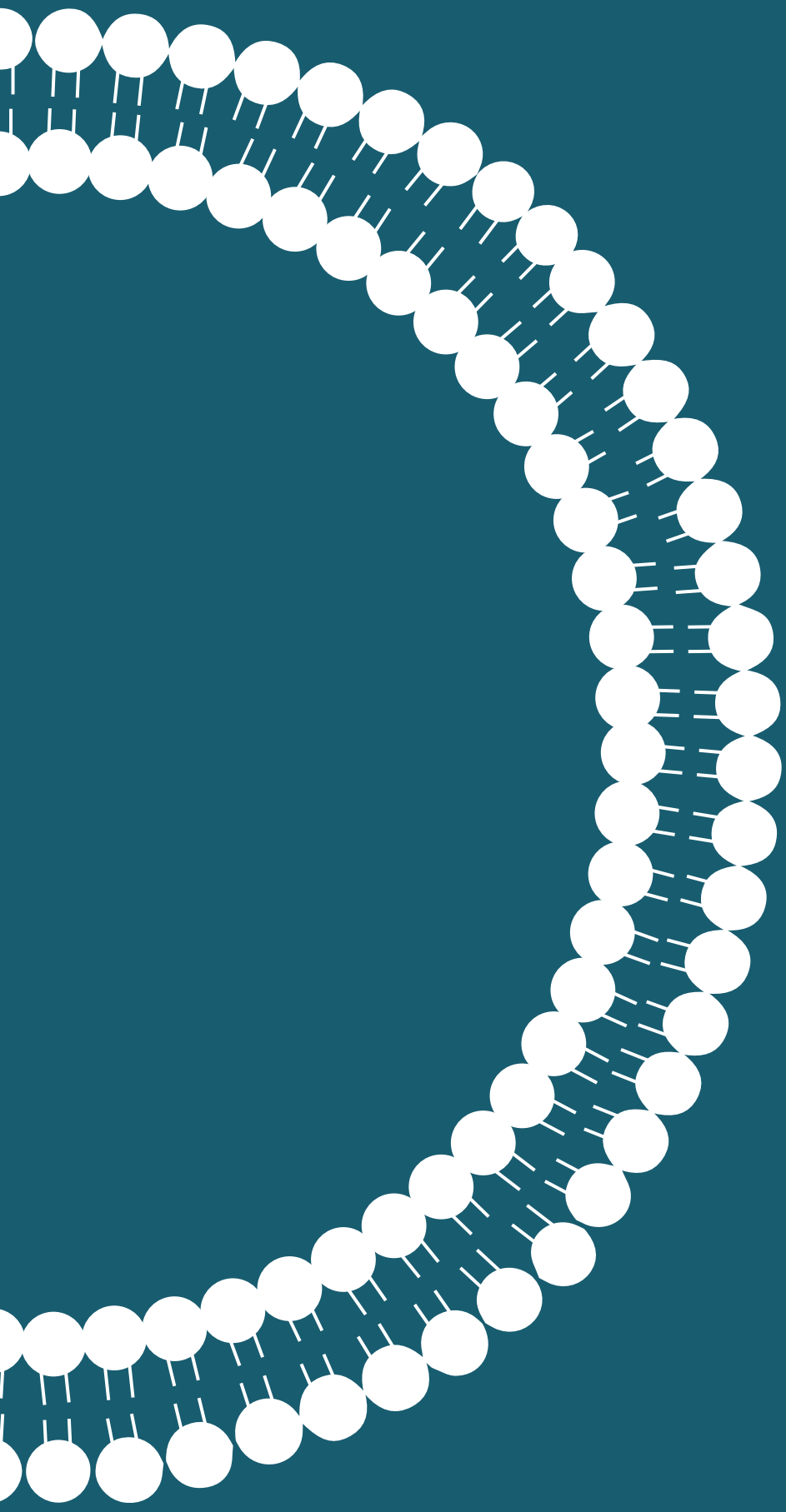

Chapter 7

Nasal subunit vaccination with cationic liposomes induces Influenza-specific resident CD8$^+$ T cells in the airways and reduces viral burden upon infection

F. Lozano Vigario[1], D. Ostroumov[2], J.A. Bouwstra[1], A. Kros[3], T.C. Wirth[2], B. Slütter[1]

[1] Division of BioTherapeutics, Leiden Academic Centre for Drug Research, Leiden University, The Netherlands
[2] Department of Gastroenterology, Hepatology, Infectious Diseases and Endocrinology, Hannover Medical School, Hannover, Germany
[3] Supramolecular & Biomaterials Chemistry, Leiden Institute of Chemistry, Leiden University, The Netherlands

Manuscript under review

ABSTRACT

The induction of anti-viral $CD8^+$ T cell immunity in the respiratory tract is key for protection against infections such as Influenza or SARS-CoV2, however most vaccines are optimized for the induction of systemic humoral immune responses. The induction of tissue-resident memory $CD8^+$ T cells via immunization can be achieved using live attenuated vaccines and it often requires a prime-boost regime with a long interval between both immunizations. Therefore, the use of safer and easier to manufacture subunit vaccines to elicit potent tissue-resident cellular immune responses is an unmet need in the vaccine field. Here, we show that intranasal immunization followed by a rapid systemic boost with a subunit vaccine based on cationic liposomes loaded with a single-epitope influenza antigen, PA224, and the adjuvant cyclic dimeric guanosine monophosphate (c-di-GMP) induces a potent and long lasting $CD8^+$ T cell response systemically and locally in the lungs. This immunization regime led to a significant reduction in viral load in lungs of influenza-infected mice. The accelerated induction of lung-resident memory $CD8^+$ T cells using a subunit vaccine can have advantages for the deployment of effective vaccines against rapidly spreading respiratory viruses.

INTRODUCTION

Respiratory viruses such as coronaviruses and influenza are a global threat for public health as seen during SARS-CoV2 pandemic and the annual epidemics of influenza. The World Health Organization (WHO) and scientific literature estimate that seasonal influenza viruses severely affect up to 5 million people every year and result in between 290,000 and 650,000 deaths[1].

Vaccination is the most effective intervention to reduce morbidity and mortality of infectious diseases. Currently used vaccines can be broadly divided into inactivated, live attenuated and subunit vaccines[2]. The focus of current vaccines is the induction of strong antibody responses, however cellular immunity is also critical for protection against viral infections[3, 4]. In the case of influenza, the generation of T cell responses against viral antigens conserved across different strains might overcome the need for annual vaccination. $CD8^+$ T cells, also called cytotoxic T cells, can recognize virus-infected cells that present viral epitopes via MHC-I molecules[5] and therefore can target antigens that are not accessible for antibodies, such as nucleoprotein- or polymerase-derived epitopes, which are substantially less prone to mutations than hemagglutinin[6]. The induction of long-term memory $CD8^+$ T cells through vaccination is therefore a key step towards the development of broadly protective influenza vaccines that do not require annual vaccination. However, the induction of immunological memory often requires a prime-boost vaccination regime with a long interval between the two immunizations, which can be an important hurdle in emergency situations such as rapidly spreading pandemics.

Additionally, in the case of respiratory viruses the induction of robust local immune responses in the respiratory mucosa is particularly important[7]. This is highlighted by the poor correlation observed between serum antibody titers and protection against influenza in a challenge study with volunteers[8]. Furthermore, despite the high efficacy in the reduction of morbidity and mortality observed for the SARS-CoV2 vaccines, these systemically administered vaccines are less effective at preventing transmission[9, 10]. One possible explanation is the low levels of local responses induced in the respiratory tract, which is the first site of infection and viral replication. Therefore, the induction of a robust tissue-resident memory T cell (T_{rm}) response in the respiratory tract can not only improve vaccine protection but also reduce viral shedding and transmission[10].

The induction of a strong local immune response in the lungs has only been achieved using live attenuated vaccines but subunit vaccines have a better safety profile, are more stable and easier to manufacture than live attenuated vaccines[11]. Furthermore, live attenuated vaccines cannot be administered to all demographic groups as they are contraindicated for immunosuppressed individuals[12]. Therefore,

the development of subunit vaccines able to induce strong and long-lasting immune responses in the respiratory tract is of urgent need.

In this study, we propose a vaccination strategy to induce influenza-specific $CD8^+$ T cells in the lungs using cationic liposomes loaded with influenza-derived $CD8^+$ T cell epitopes and bis-(3'-5')-cyclic diguanylate monophosphate (c-di-GMP). C-di-GMP is cyclic dinucleotide that can induce type I interferon production by activating the stimulator of interferon genes (STING) signal pathway and it has been studied as an adjuvant in cancer vaccines[13, 14]. Cationic liposomes have previously been shown to induce strong antigen-specific $CD8^+$ T cell responses[15]. Apart from their immune activating properties, cationic liposomes present advantages for intranasal vaccination such as the favourable electrostatic interaction with the negatively charged mucosal lining that promotes mucoadhesion[16]. Previous studies showed that the delivery of an intranasal influenza vaccine using a mucoadhesive gel induced stronger and faster antibody responses both in the mucosa and systemically compared to soluble controls[17].

Here, we show that the c-di-GMP-loaded cationic liposomes can be used as a platform to induce strong $CD8^+$ T cell responses against a variety of peptide antigens derived from SARS-CoV2 and influenza. Furthermore, we use liposomes loaded with an influenza-derived antigen in an accelerated prime-boost regime[18, 19] consisting of a nasal prime followed by a systemic boost and show that this immunization strategy induces a strong and durable $CD8^+$ T cell response both systemically and in the lungs and it leads to a reduction of viral load in lungs of mice after influenza challenge.

MATERIALS

Lipids 1,2-distearoyl-sn-glycero-3-phosphocholine (DSPC), 1,2-dipalmitoyl-3-trimethylammonium-propane (DPTAP) were purchased from Avanti Polar Lipids (Alabaster, AL, USA). Cholesterol was obtained from Sigma-Aldrich (Zwijndrecht, the Netherlands). Adjuvant bis-(3'-5')-cyclic dimeric guanosine monophosphate (c-di-GMP) was purchased from Invivogen (San Diego, CA, USA). Peptides were purchased from GenScript Biotech (Rijswijk, the Netherlands). The agonistic anti-CD40 antibody (clone 1C10, hybridoma) was kindly provided by Frances Lund, Department of Microbiology, University of Alabama at Birmingham, AL, USA. The antibodies Thy1.2 (CD90.2)-PE-Cy7, CD8a-PE-Dazzle 594, CD8a-Brilliant Violet 510, CD8a-FITC, IFNγ-APC, CD69-PE, CD103-Brilliant Violet 510, CD4-APC, Ly6G-PerCP, F4/80-Brilliant Violet 650 were purchased from Biolegend (CA, USA). The antibodies CD8a-FITC, CD8a-PE, IFN-γ-eFluor450, TNF-α-PE, CD69-FITC, CD103-FITC, CD4-eFluor450, Ly6C-PE, CD11b-APC, CD19-FITC and Fixable

Viability Dye-APC-eFluor780 were purchased from eBioscience (ThermoFisher Scientific, MA, USA).

A/PR/8/34 H1N1 (PR8 H1N1) virus was a kind gift from Dr. A. Huckriede (UMC Groningen, NL)[20]. Stock solutions in allantoic fluid (2.7 x 10^9 TCID50/ml) were thawed on ice and diluted in cold PBS to 20,000 TCID50/ml before nasal administration into mice.

METHODS

SARS-CoV2 peptide antigen selection

For the selection of SARS-CoV2-derived peptides to load into the cationic liposomes, we screened the amino acid sequence of the virus surface glycoprotein (NCBI Reference Sequence: YP_009724390.1) and the nucleocapsid phosphoprotein (NCBI Reference Sequence: YP_009724397.2) and selected previously described[21], conserved epitopes with high predicted binding affinity for HLA-A*11:01.

Preparation of cationic liposomal formulations

Liposomes were prepared using the lipid film hydration method as previously described[22]. Briefly, a total of 10mg of DSPC, DPTAP and cholesterol dissolved in chloroform were mixed in a round-bottom flask in a molar ratio of 4:2:1 (DSPC:DPTAP:CHOL). The lipids were mixed with 200μg of bis-(3'-5')-cyclic dimeric guanosine monophosphate (c-di-GMP). The organic solvent was removed by means of a rotary evaporator with pressure set at 180 mbar and connected to a water bath at 40°C. The dry lipid film was hydrated with 1 mL of either milliQ water or 500 μg of peptide dissolved in milliQ water. The resulting suspension of multilamellar vesicles was snap-frozen using liquid N_2 and freeze-dried overnight using a Christ alpha 1-2 freeze-dryer (Osterode, Germany). The dry product was re-hydrated stepwise by first adding 25% of the final volume of phosphate buffer (PB) 10 mM pH 7.4 followed by vortex and 30 minutes incubation at 60°C in a water bath. This step was repeated one more time. A final re-hydration step involves the addition of the remaining 50% of the final volume of PB 10mM pH 7.4, vortex and incubation in 60°C water bath for at least 1 hour. The lipid concentration after re-hydration was 5 mg/mL. The formulation was down-sized by means of high-pressure extrusion using a LIPEX Extruder (Northern Lipids Inc., Canada) connected to a water bath at 60°C. Formulations were extruded 4x through 400nm and 200nm stacked track-etched polycarbonate membranes (Whatman® Nucleopore™, GE Healthcare, Little Chalfont, UK). The resulting monodisperse formulations were purified using Vivaspin centrifugal concentrators (MWCO 100 kDa, Sartorius, Göttingen, Germany) to remove non-encapsulated peptides and c-di-GMP. Finally,

formulations for intranasal administration were further concentrated using a N_2 gas flow.

Characterization of the formulations

The z-average hydrodynamic diameter (Z_{ave}), polydispersity index (PdI) and ζ-potential of the formulations were determined using dynamic light scattering (DLS) and laser Doppler electrophoresis in a Zetasizer NanoZS (Malvern Panalytical, UK).

Peptide and c-di-GMP concentrations were determined by reverse-phase ultra-high performance liquid chromatography (UPLC). For quantification of the peptides, a modified Bligh-Dyer method was used to extract and separate the peptide from the liposomes. In short, 100 μL of formulation was mixed with 250 μL of methanol, 250 μL of 0.1M hydrochloric acid 0.1M and 250 μL of chloroform. The mix was vortexed for 30 seconds and centrifuged for 10 minutes at 1000G. A sample was taken from the water-methanol upper phase containing the peptides. The extracted sample was analysed by injecting 10 μL of sample into a 1.7 μm BEH C18 column (2.1 x 50 mm, Waters ACQUITY UPLC, Waters, MA, USA). Column temperature was set at 40°C. A mobile phase linear gradient was applied to the column starting with 95% milliQ water with 0.1% TFA (solvent A) and 5% acetonitrile with 0.1% TFA (solvent B) and going to 95% solvent B in 7 minutes. The gradient was followed by 95% solvent B for 2 minutes and back to 95% solvent A for 3 minutes. Flow rate of the mobile phase was set at 0.5 mL/min. Peptides were detected by absorbance at 220 nm using ACQUITY UPLC TUV detector. To quantify the c-di-GMP concentration in the formulations, 10 μL of the liposomal formulation was directly injected into a 1.7 μm BEH C18 column (2.1 x 50 mm, Waters ACQUITY UPLC, Waters, MA, USA), without previous sample pre-treatment. The mobile phases and the gradient applied were the same as for quantification of the peptides. The detection of c-di-GMP was done by absorbance at 254 nm using ACQUITY UPLC TUV detector.

Animals

Mice were bred in the Animal Research Facility of Leiden University, Faculty of Science, The Netherlands or the Animal Care Facility of Hannover Medical School, Germany, under standard laboratory conditions. Animals were provided with food and water *ad libitum.* Animal experiments were reviewed and approved by the Ethics Committee for animal experiments of Leiden University or by German institutional and government boards (LAVES). Animal work was performed according to Dutch and/or German Government regulations and Directive 2010/63/EU of the European Parliament.

In vivo screening of antigen-specific immune responses to SARS-CoV2-derived antigens

Transgenic mice expressing human HLA-A11 were immunized intravenously with a mix of liposomes loaded with 5 μg of c-di-GMP and 10 nmol of the SARS-CoV2-derived peptides COVN361, COV1020, COVN134, COVS757 and COVN310 (peptides details in Supplementary Table 1). After 1 week, mice received an intravenous boost with a mix consisting of 50 nmol of each of the SARS-CoV2 peptides, 5 μg c-di-GMP and 50 μg of agonistic anti-CD40 antibody. Blood was collected via submandibular bleeding on day 7 (after prime) and day 27 (after boost) for *ex vivo* restimulation with the individual peptides and flow cytometry analysis. Epitope-specific $CD8^+$ T cell response was investigated by intracellular IFNγ staining as previously described[23, 24]. Briefly, stimulation of peptide-specific T cells was performed by incubation of cell suspensions with the respective SARS-CoV2-derived peptides (2 μg/ml) in presence of GolgiPlug (1/1000 dilution) (Becton Dickinson, San José, CA, USA) in RPMI medium (Gibco), supplemented with 10% FCS (Gibco), penicillin (50 U/ml), streptomycin (50 µg/ml) (Bio&Sell). Unstimulated T cells in presence of GolgiPlug were used as control for background cytokine production. Cells were incubated overnight at 37°C and 5% CO_2. Prior to staining, cells were treated with TruStain FcX (Biolegend) to block Fc-receptors for 15 minutes at 4°C, then stained for CD8a-FITC (53–6.7), IFNγ-APC (XMG1.2), TruStain FcX (anti-mouse CD16/32) and CD90.2 (53-2.1). Samples were analysed by flow cytometry data in a FACSCanto II (BD Bioscience, Heidelberg, Germany).

In vivo evaluation of Influenza-specific immune responses

C57Bl6/J mice between 8 and 12 weeks old were weighted before the start of the experiments and randomly allocated to the different control or experimental groups using the randomization software RandoMice® and using weight as a blocking factor for the randomization method[25]. On day 1, animals were immunized with DSPC:DPTAP:Cholesterol liposomes containing 10 nmol of the murine immunodominant influenza epitopes $PA_{224-233}$ (PA224) [26] and $NP_{366-374}$ (NP366) [27] peptides and 5 μg of c-di-GMP. Animals received 10 μL of formulation intranasally, 100 μL of formulation intravenously through the tail vein or subcutaneous under the skin over the neck. For intranasal immunizations mice were lightly anaesthetized with 0.6 L/min of 4% isoflurane. On day 7, a blood sample of 50-100 μL was taken from the animals by tail vein cut, and 200 μL of either DSPC:DPTAP:Cholesterol liposomes containing the peptide(s) antigen(s) and c-di-GMP or a boost mix containing antiCD40 agonistic antibody (clone 1C10, hybridoma provided by Frances Lund, Department of Microbiology, University of Alabama

at Birmingham, AL, USA), c-di-GMP, and peptides was administered intravenous through the tail vein. At the end of the experiment, mice received an intravenous injection of 3 μg of anti-mouse antiCD45.2-Allophycocyanin (antiCD45.2-APC) in order to label all T cells in circulation, therefore allowing the identification of tissue-infiltrated T cells from circulating T cells as previously described[28]. Mice were sacrifice by cervical dislocation 3 minutes after antiCD45.2-APC injection. After sacrifice, spleen, lungs, and inguinal lymph nodes were collected for *ex vivo* restimulation and flow cytometry analysis.

In vivo challenge of vaccinated mice with PR8 H1N1

Based on the results from the previous experiment, we chose the most optimal prime immunization route, antigen and boost formulation to vaccinate mice and subsequently challenge them with influenza virus. Mice between 8 and 12 weeks old were weighted and randomly allocated to either treatment or control group. Mice in treatment group received an intranasal or subcutaneous immunization DSPC:DPTAP:Cholesterol liposomes containing 10 nmol of PA224 antigen peptide and 5 μg of c-di-GMP, while mice in the control group received an intranasal immunization with the same cationic liposomal formulation containing 5 μg c-di-GMP but no antigen peptide or intranasal PBS. Intranasal immunizations were performed as described above. On day 7 after prime immunization, a blood sample was drawn via tail vein cut and mice received an intravenous injection of DSPC:DPTAP:Cholesterol liposomes containing either 10 nmol of PA224 and 5 μg of c-di-GMP (treatment group) or 5 μg c-di-GMP only or PBS (control group). On day 14, 50-100 μL blood sample was taken via tail vein cut. On day 35 mice were weighted to determine baseline weight before viral challenge. For the viral challenge, mice were lightly anaesthetized with 0.6 L/min of 4% isoflurane and a 50 μL suspension containing 1000 $TCID_{50}$ (median tissue culture infectious dose) of PR8 H1N1 was applied to the nostrils. After viral challenge mice were weighted daily and sacrificed on day 39 by cervical dislocation. Lungs were collected for viral titer quantification and *ex vivo* T cell restimulation. Lung samples were mechanically disrupted and digested with collagenase and DNAase I enzymes for 30 minutes at 37°C. Digested samples were passed through a cell strainer and immune cells were isolated using 35% Percoll density gradient centrifugation, followed by *ex vivo* restimulation with PA224 and flow cytometry staining. Spleens were restimulated *ex vivo* with PA224, stained for flow cytometry. BAL samples were directly stained for Thy1.2-PE-Cy7, CD8a-Brilliant Violet 510, CD4-eFluor450, Ly6G-PerCP, Ly6C-PE, CD11b-APC, CD19-FITC and fixable viability dye APC-eFluor 780 and analysed by flow cytometry in Cytoflex S (Beckman Coulter, CA, USA).

Ex vivo restimulation and flow cytometry analysis of samples

Prior to restimulation, organ samples were processed into a single cell suspension. Spleen, lungs and blood samples were lysed using Ammonium-Chloride-Potassium (ACK) lysing buffer. Samples were stimulated with either 5 μg/mL of peptide and 3 μg/mL of Brefeldin A (BrefA) or only 3 μg/mL of BrefA (unstimulated control) for 5 hours at 37°C and using bone marrow derived dendritic cells as feeder cells. After stimulation, blood samples were stained for Thy1.2-PE-Cy7, CD8a-FITC, IFNγ-eFluor450 and fixable viability dye APC-eFluor780 and analysed by flow cytometry in Cytoflex S (Beckman Coulter, CA, USA). Spleen, lymph nodes and lung samples were stained for Thy1.2-PE-Cy7, CD8a-PE, CD4-APC, CD69-FITC, CD103-Brilliant Violet 510, IFNγ-eFluor450 and fixable viability dye APC-eFluor780 and analysed by flow cytometry in Cytoflex S (Beckman Coulter, CA, USA).

Measurement of viral titers

Lung samples for measurement of viral titer were mechanically homogenized using glass mortar and pestle in guanidine thiocyanate (GTC) immediately after collection of the organ and store at -80°C until the quantification of viral titers was performed. RNA was isolated from samples using phenol/chloroform extraction. The RNA was concentrated further using a mini-prep column. RNA to cDNA transcription was performed using RevertAid M-MuLV reverse transcriptase according to manufacturer instructions. Quantitative viral gene determination was performed using SYBR Green Master Mix on QuantStudio 6 Flex (Applied Biosystems, Life Technologies). Standard curve was prepared with known viral titers and used to quantify the viral load in lung tissue.

Statistical analysis

Statistically significant difference between conditions was assessed by one-way ANOVA followed by Tukey's multiple comparison test, two-way ANOVA followed by Sidak multiple comparisons test or two-tailed unpaired t-test. P-values lower than 0.05 were considered significant. Software used for statistical analysis was GraphPad Prism 9.3.1 for Windows (GraphPad Software, California, USA).

RESULTS

Intravenous prime-boost regime induces a potent antigen-specific CD8+ T cell response to a variety of peptide antigens

Table 1. Physicochemical characteristics of liposomal formulations. Data shown represents the average ± standard deviation of at least two separate batches of formulation (n ≥ 2).

Formulation	Z_{ave} (nm)	PDI	ζ-potential (mV)	LE% peptide
DSPC:DPTAP:CHOL:cdiGMP	178.1±2.68	0.11±0.031	33.25±2.53	-
DSPC:DPTAP:CHOL:cdiGMP:PA224	194.0±15.62	0.097±0.053	29.01±5.29	2.51
DSPC:DPTAP:CHOL:cdiGMP:NP366	223.1±8.75	0.064±0.024	27.90±1.18	8.12
DSPC:DPTAP:CHOL:cdiGMP:COVN361	218.0±16.26	0.085±0.056	32.39±0.68	4.97
DSPC:DPTAP:CHOL:cdiGMP:COVS1020	206.4±11.58	0.062±0.018	31.52±0.88	7.66
DSPC:DPTAP:CHOL:cdiGMP:COVN134	202.6±16.64	0.083±0.020	30.26±2.27	6.15
DSPC:DPTAP:CHOL:cdiGMP:COVS757	201.2±20.45	0.15±0.082	30.28±1.18	8.71
DSPC:DPTAP:CHOL:cdiGMP:COVN310	207.1±8.225	0.11±0.034	31.12±2.67	3.23

To study the capacity of the cationic liposomal formulations (physicochemical properties in Table 1) to induce virus-specific CD8+ T cell responses *in vivo*, we immunized mice with cationic liposomes loaded with a variety of different peptide antigens derived from SARS-CoV2 or H1N1 influenza. One week after prime immunization mice received a boost with a mix of antiCD40 antibody, c-di-GMP and free peptides, to expand potential low frequency responses[19]. We observed a strong CD8+ T cell response against the epitopes COVN361 and COVN134 from SARS-CoV2 in blood of vaccinated mice after prime-boost regime but only weak or no detectable responses against the other three antigens COVS1020, COVS757 and COVN310 (Figure 1C). In the case of mice immunized with cationic liposomes loaded with the influenza peptides PA224 and NP366, we observed a strong CD8+ T cell response against PA224 but only a minimal response for NP336 after prime immunization. Following boost immunization with antiCD40, c-di-GMP and free peptides, the PA224-specific CD8+ T cell response had massively expanded, however again the NP366-specific response in spleen of mice after prime and boost was close to undetectable (Figure 1D). Thus, this subunit vaccine formulation allows expansion of a selection of SARS-CoV2 and influenza specific CD8+ T cells.

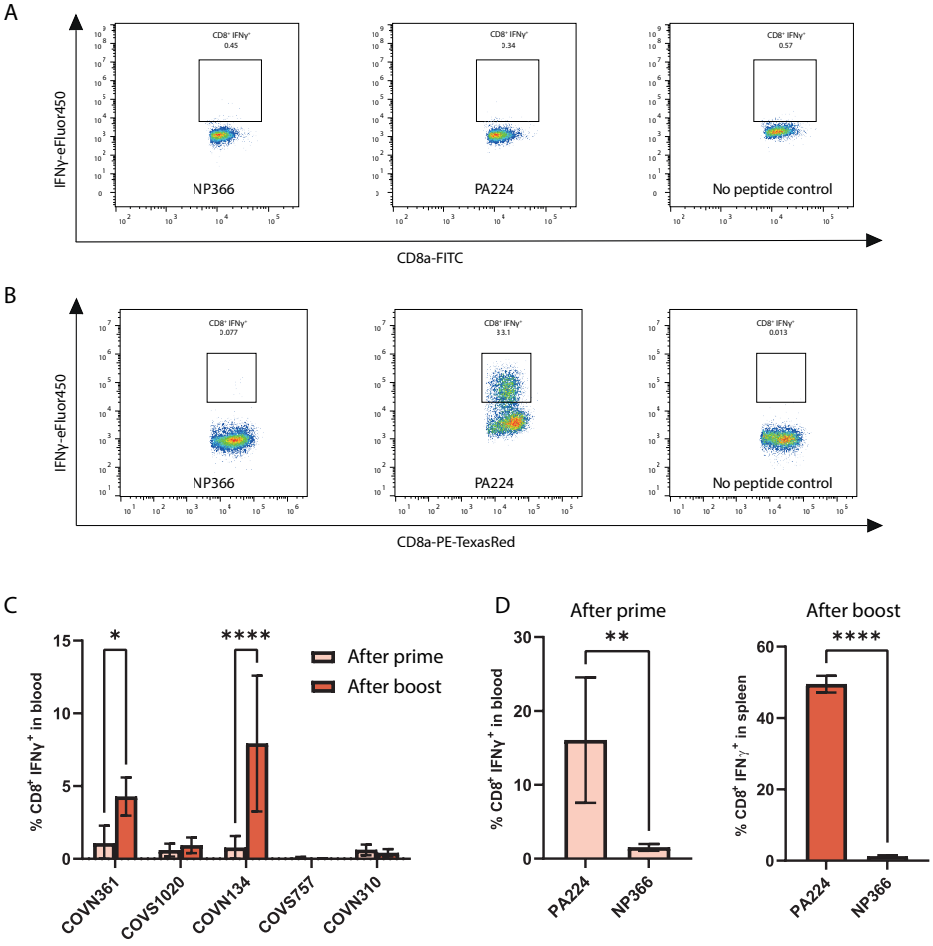

Figure 1. Immune responses after immunization with viral peptide-loaded cationic liposomes. (A) Representative flow cytometry plots of blood-derived CD8+ T cells after prime and before boost restimulated with NP366, PA224 or no peptide as control. (B) Representative flow cytometry plots of spleen-derived CD8+ T cells on day 27 after boost restimulated with NP366, PA224 or no peptide as control. (C) SARS-CoV2-specific CD8+ T cell response in blood after prime and after 27 days after boost with antiCD40, peptide and c-di-GMP. (D) Influenza-specific CD8+ T cell response in blood after prime and in spleen on day 30 after boost. * $p < 0.05$, ** $p < 0.01$, **** $p < 0.0001$ determined using (A) two-way ANOVA followed by Sidak multiple comparisons test or (B) two-tailed unpaired t-test.

Intravenous, intranasal and subcutaneous prime immunization followed by systemic boost induce a potent and long lasting CD8+ T cell response

As systemic intravenous (IV) administration is not a preferred administration route and does not lead to effective establishment of lung T_{rm}[29], we next aimed to address whether the cationic subunit vaccine may induce antigen-specific $CD8^+$ T cells response through local administration routes. We compared IV, intranasal (IN) and subcutaneous (SC) prime with c-di-GMP and PA224-loaded cationic liposomes. Control mice received empty liposomes intranasally. After prime immunization, all mice (including the control group) received an IV boost with antiCD40 antibody, c-di-GMP and PA224. After IV priming, only the IV and SC route induced detectable $CD8^+$ T cell response in blood. Thirty days after boosting, all groups showed massive expansion of PA224-specific $CD8^+$ T cells in the spleen (Figure 2B), lungs (Figure 2C) and lymph node (Figure 2D), revealing that the liposomal formulation is not restricted to IV use. Interestingly, the percentage of PA224-specific T cells expressing CD103 was significantly higher in the IN-immunized mice compared to SC or IV groups (Figure 2E), suggesting that a larger fraction of the cells are T_{rm} cells. As we have previously shown that IV boosting may expand the number of locally induced T_{rm}[30], we evaluated the number of PA224-specific $CD8^+$ T cells in the lung parenchyma after boosting, using the intravascular staining protocol to exclude $CD8^+$ T cells in the capillary beds. Indeed, the percentage of lung-infiltrated $CD8^+$ T cells was significantly higher in the IN prime group compared to systemic immunization (Figure 2F). Overall, this data indicates that an IN prime with cationic liposomes induces a systemic $CD8^+$ T cell response and a local response in the lungs with characteristics of tissue-resident $CD8^+$ T cells.

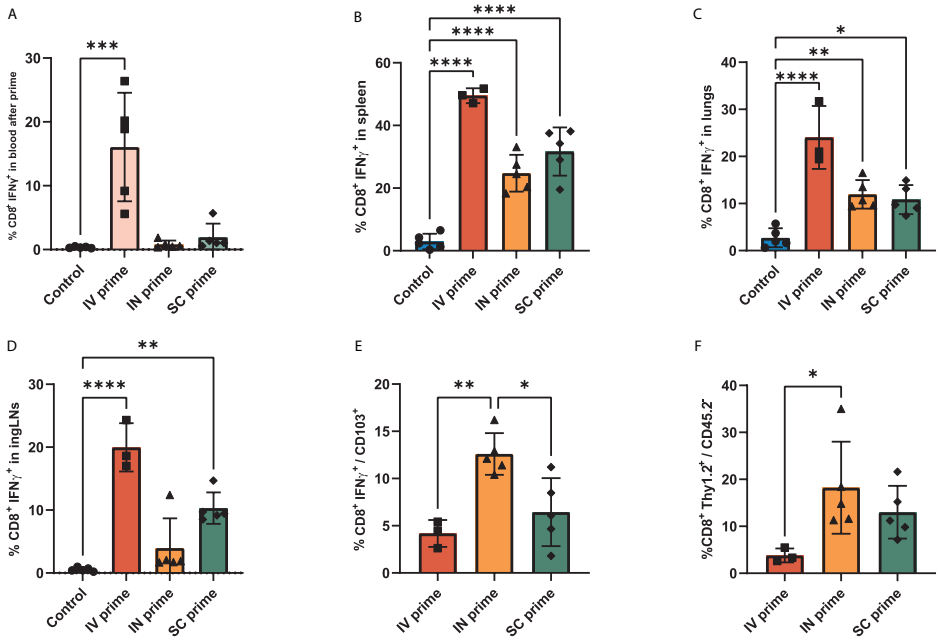

Figure 2. CD8+ T cell responses to PA224 after prime through different administration routes. (A) PA224-specific CD8+ T cell responses in blood after prime and before boost immunization. PA224-specific CD8+ T cell response in (B) spleen, (C) lungs and (D) inguinal lymph nodes on day 30 after boost. (E) PA224-specific CD8+ T cells expressing CD103 in lungs. (F) Lung-resident CD8+ T cells identified by lack of staining with antiCD45.2-APC administered IV shortly before sacrifice. * $p < 0.05$, ** $p < 0.01$, *** $p < 0.001$, **** $p < 0.0001$ determined using one-way ANOVA followed by Tukey's multiple comparison test.

Both heterologous and homologous prime-boost strategies induce strong CD8⁺ T cell responses

Although the antiCD40-based boost mix was able to induce a potent CD8⁺ T cell response, the use of monoclonal antibodies in prophylactic vaccines has several limitations in terms of cost, manufacture and side effects[31]. Therefore, we next compared the CD8⁺ T cell response elicited by this heterologous prime-boost regime versus a homologous prime-boost regime where both prime and boost consist of the cationic liposomal formulation. Control mice did not receive prime or boost immunizations. We observed that both immunization regimes were able to induce a potent PA224-specific CD8⁺ T cell response in both spleen (Figure 3A) and lungs (Figure 3B) after intranasal prime followed by intravenous boost, however higher variation in the response was observed in the liposome boost group (SD = 15.92) compared to the antiCD40 boost group (SD = 4.89). No significant differences

were found between the two prime-boost regimes in the frequency of CD103 in the PA224-specific CD8⁺ T cell population (Figure 3C). This data indicates that both homologous and heterologous prime-boost strategies induce similar CD8⁺ T cell responses systemically and locally in the lungs.

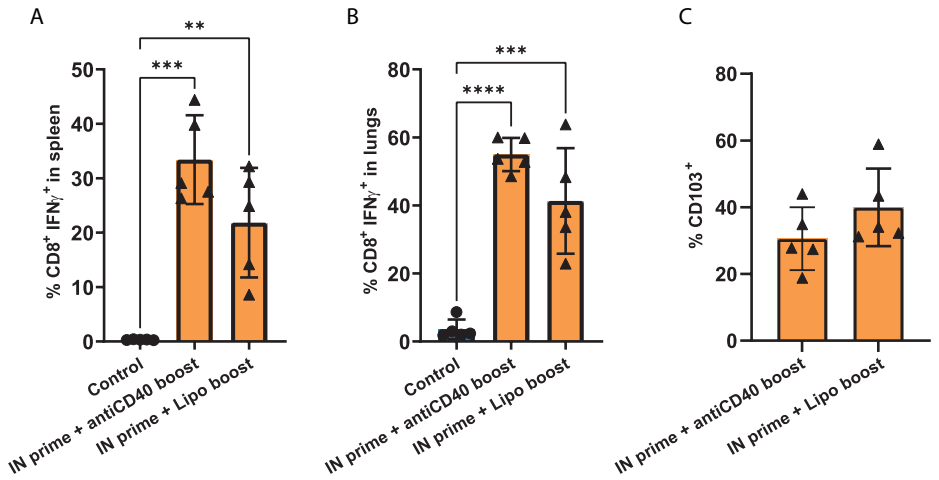

Figure 3. Comparison of boost immunization with either antiCD40 boost mix or cationic liposomes after intranasal prime. PA224-specific CD8+ T cell response in (A) spleen and (B) lungs on day 7 after boost. (C) Frequency of CD103 in PA224-specific (IFNγ+) CD8+ T cells in the lungs. ** $p < 0.01$, *** $p < 0.001$, **** $p < 0.0001$ determined using one-way ANOVA followed by Tukey's multiple comparison test.

Response to intranasal immunization correlates with a reduction in lung viral titers upon Influenza infection

After confirming that the prime and boost immunizations with cationic liposomes was able to induce a systemic PA224-specific CD8⁺ T cell response, including a strong response in the lungs, we aimed to determine if these CD8⁺ T cells are able to reduce the viral load in the lungs after challenge with PR8 H1N1 virus. Mice received an IN prime immunization with either cationic liposomes loaded with c-di-GMP (control) or liposomes loaded with PA224 and c-di-GMP (vaccinated), followed by systemic boost with the same formulation 7 days later. On day 35 of the experiment (27 days after boost immunization), mice were challenged with a lethal dose of H1N1 PR8 (1000 TCID50) and 4 days later they were sacrificed. The results from blood samples taken before (Figure 4A) and after (Figure 4B) boost confirm a significant increase in PA224-specific CD8⁺ T cells in the vaccinated group compared to control at 7 days after boost. Furthermore, the vaccinated group showed a strong PA224-specific CD8⁺ T cell response in the lungs (Figure 4C). The reduction in body weight

in all the mice confirmed that the infection was successful, with no significant differences in weight loss between groups (Figure 4D). Lung viral titers on day 4 after infection trended downward but were not significantly different between vaccinated and control groups, due to 3 non-responders in vaccinated group (Figure 4E). Viral titers however showed a clear negative correlation with the CD8⁺ T cell response elicited after booster immunization (Figure 4F).

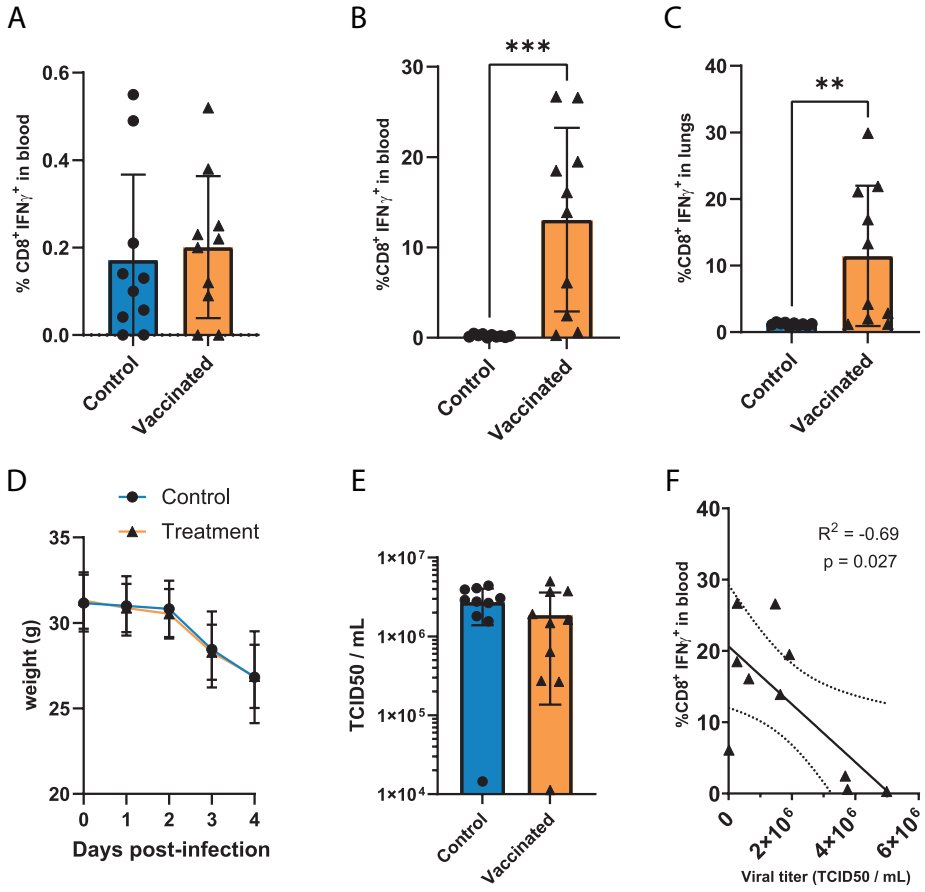

Figure 4. Challenge experiment. (A) CD8+ T cell response before and (B) after boost. (C) PA224-specific CD8+ T cell response in lungs. (D) Weight post infection. (E) Viral titers in lungs 4 days after infection and (F) correlation between lung viral titers and systemic CD8+ T cell response after boost. ** $p < 0.01$, *** $p < 0.001$ determined using one-way ANOVA followed by Tukey's multiple comparison test. Correlation p-value and r correlation coefficient determined using Person's correlation test.

Local CD8+ T cell response after intranasal immunization reduces viral burden upon influenza infection

To determine the role of the local and systemic influenza specific CD8+ T cell response in the viral burden reduction, we next compared the viral loads 4 days after infection in intranasally primed versus subcutaneously primed mice. Control mice were primed with intranasal PBS and boost IV with PBS. Mice primed subcutaneously showed a stronger systemic immune response both one week after boost (Figure 5A) and immediately before the infection (Figure 5B) compared to the intranasal group, suggesting the systemic PA224-specific memory CD8+ T cell response was larger in the SC versus the IN vaccinated mice. After infection animals in all groups lost a significant percentage of body weight (Figure 5C), indicating a successful viral infection. Interestingly, we observed a significant decrease in viral load in the group that received cationic liposomes intranasally compared to the control, but this protective effect was not observed in mice primed subcutaneously (Figure 5D). When comparing the viral load to the PA224-specific CD8+ T cell response elicited by the formulations in the IN group, we observed an inverse correlation (Figure 5E) while no correlation was present in the group immunized subcutaneously (Figure 5F). Thus, although the IN vaccination led to a smaller systemic virus-specific CD8+ T cell response, the induction of local T_{rm} appear to provide superior protection against H1N1 PR8 infection. Indeed, the bronchoalveolar lavage (BAL) fluid, which can be used as a proxy to study the inflammatory state of lungs upon infection[32], showed change in the leukocyte composition. The cell composition of the BAL of immunized mice on day 4 after infection showed no differences between control and vaccinated mice in terms of granulocytes (Figure 6A) or monocytes/macrophages (Figure 6B). A significant increase in B cell content of in the SC prime group could be observed compared to both control and IN groups (Figure 6C). Similarly, the BAL showed an increase in lymphocytes in the SC group compared to control (Figure 6D). When looking at the two major T cell subsets, we observed an increase in CD4+ T cells in the IN group compared to SC primed mice (Figure 6E). Finally, both IN and SC groups showed significantly higher percentages of CD8+ T cells in the BAL compared to control (Figure 6F). Overall, this data shows that immunized mice present an enhanced recruitment of T cells to the lungs upon infection, with the response mainly driven by CD8+ T cells.

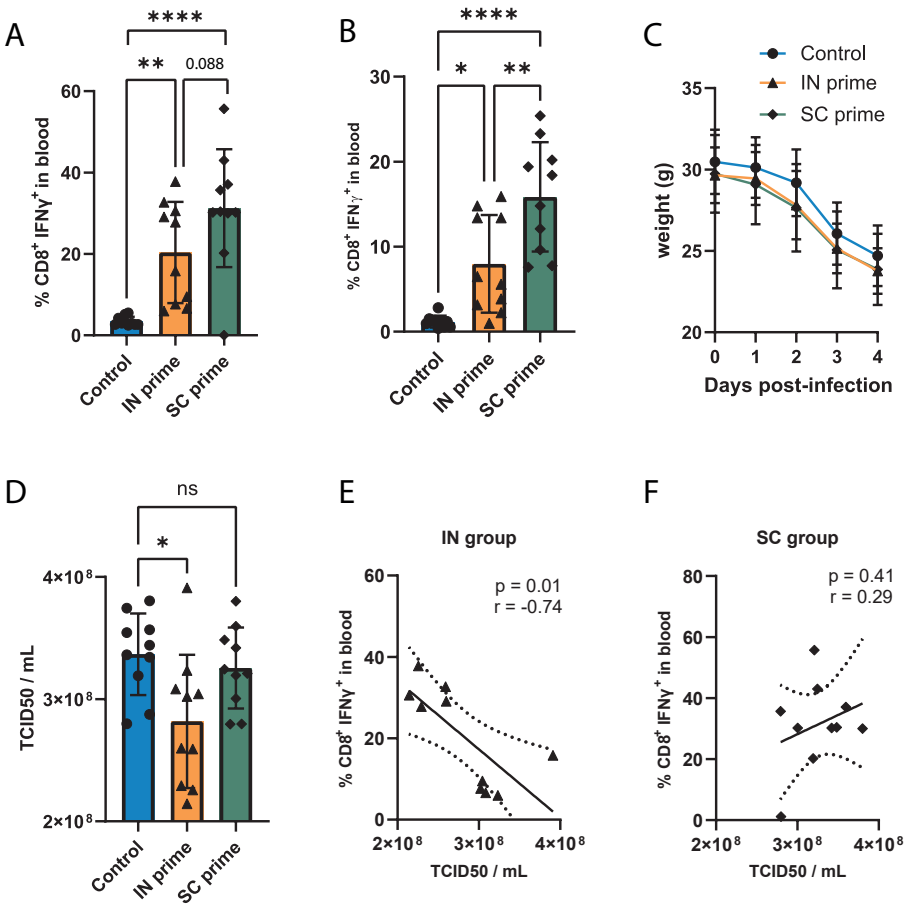

Figure 5. Viral challenge after intranasal and subcutaneous immunizations. PA224-specific CD8+ T cell responses in blood (A) on day 7 and (B) before infection on day 27 after boost. (C) Mice weight post infection. (D) Viral titers in lungs 4 days after infection. Correlation between lung viral titers and PA224-specific CD8+ T response after boost in (E) intranasal group and (F) subcutaneous group. * $p<0.05$, ** $p < 0.01$, **** $p < 0.0001$ determined using one-way ANOVA followed by Tukey's multiple comparison test. P-value and r correlation coefficient determined using Person's correlation test.

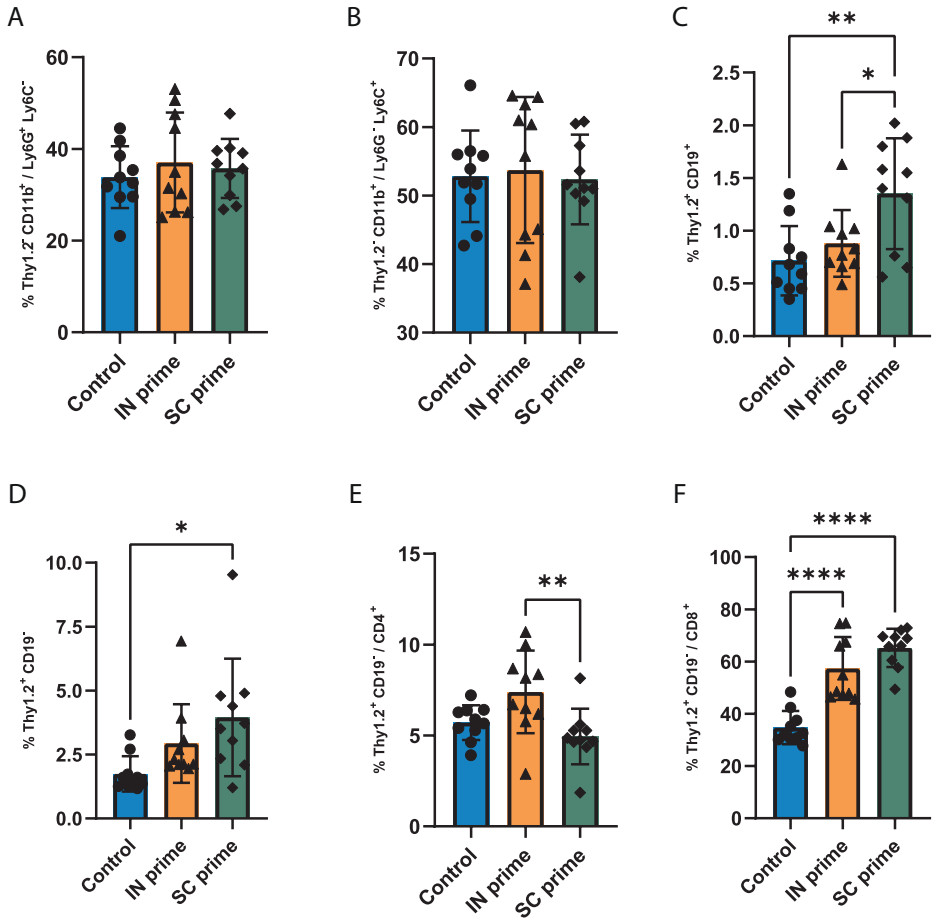

Figure 6. Cell composition of bronchoalveolar lavage (BAL) of immunized and control mice. Percentage of (A) granulocytes (Ly6G+ Ly6C-) and (B) monocytes (Ly6G- Ly6C+) in the myeloid cell compartment in BAL. (C) Percentage of B cells. (D) Percentage of T cells in live cell population in BAL. Percentage of (E) CD4+ T cell subset and (F) CD8+ T cell subset within the T cell population. * $p<0.05$, ** $p < 0.01$, **** $p < 0.0001$ determined using one-way ANOVA followed by Tukey's multiple comparison test.

DISCUSSION

Vaccine efficacy has traditionally been measured by the capacity to induce potent antibody responses, while the induction of cellular immunity has been a secondary goal. However, recent studies have highlighted the importance of T cell responses for long-lasting protection against viral infections[3, 33]. The induction of cellular

immunity in addition to the antibody response could overcome the problem of virus variants that escape humoral immunity due to the high mutation rates of certain proteins such as hemagglutinin in Influenza virus[34]. Cytotoxic $CD8^+$ T cells are key players in anti-viral cellular immunity since they can directly kill infected cells. $CD8^+$ T cells can recognize antigenic epitopes that are usually not accessible to antibodies, and they often target more conserved epitopes of the virus, such as those derived from the nucleoprotein or the virus polymerase[34]. Furthermore, the generation of these immune responses locally in the respiratory tract, in the form of virus-specific T_{rm} responses, is crucial for protection and could reduce transmission of respiratory viruses like influenza and coronaviruses[10]. Cellular immunity can be achieved through vaccination with live attenuated vaccines, however the safer and easier to manufacture subunit vaccines are not so efficient at inducing T cell responses.

Here, we show that a subunit vaccine consisting of cationic liposomes loaded with c-di-GMP and a single-epitope antigen induces a potent, long-lasting and antigen-specific $CD8^+$ T cell response both systemically and locally in the lungs against different antigen peptides derived from SARS-CoV2 and influenza. Furthermore, $CD8^+$ T cells in the lungs of intranasally primed mice showed higher expression of CD103 (Figure 2F and 3C), a common marker of memory $CD8^+$ T cells and we showed an increase in lung-resident $CD8^+$ T cells in this group using intravascular CD45.2 staining (Figure 2E). While the generation of this type of cellular immunity often requires long intervals between prime and boost[35, 36], we show that this vaccine formulation can induce long-lasting memory $CD8^+$ T cells after an accelerated prime-boost regime. Translated to humans, this rapid induction of a potent memory T cell response can have logistics advantages for prompt and efficient immunization against new pandemic virus strains of influenza or SARS-CoV2.

The lack of response against some of the peptides tested (Figure 1) indicates that the selection of appropriate viral epitopes during early stages of vaccine design is key. In this study, we compared two different epitopes from influenza virus, PA224 derived from the virus polymerase acidic protein, and NP366 derived from the viral nucleoprotein. Although T cell immunity in primary influenza infections in C57Bl/6 mice seems to be almost equally divided between NP366-specific $CD8^+$ T cells and PA224-specific $CD8^+$ T cells[37], in our experiments PA224 epitope induced stronger $CD8^+$ T cell responses compared to NP366. Antigenic competition might explain the weak immune responses towards some of the SARS-CoV2 epitopes and previously reported immunogenic epitopes such as NP366[38]. Future studies should take in to account this effect of antigenic competition for the selection of peptide antigens and the design of administration strategies[39].

In previous studies, a heterologous prime-boost regime where prime immunization consisted of cationic liposomes and boost was performed with agonistic antiCD40 monoclonal antibody mixed with antigens and adjuvants has proven to induce a strong $CD8^+$ T cell response against tumour antigens[40]. Here, we show that prime and boost can be performed with the same liposomal formulations leading to a comparable immune response (Figure 3). This could have advantages in terms of affordability of such vaccines for both viral infections and cancer since it circumvents the need to use costly monoclonal antibodies. Furthermore, side effects associated to antiCD40 antibodies, such as cytokine storm, could be acceptable in the context of anti-cancer therapies but not for prophylactic vaccination[41]. Future research should investigate the source of the increased variability on the elicited immune response when boost was performed with cationic liposomes in comparison to the agonistic antiCD40 boost mix and the formulation should be optimized further to reduce this variability.

We show that intranasal prime is key for this viral burden reduction (Figure 5D and 5E) since subcutaneously primed mice showed comparable viral titers to the control group despite the stronger systemic immune response in this group (Figure 5A and 5B). These results are in line with previous studies that have shown that $CD8^+$ T cell responses induced by intranasal vaccination with non-replicating adjuvanted vaccine are protective against influenza infections, in contrast with the $CD8^+$ T cell responses induced through subcutaneous immunization[35]. The improved capacity of intranasally administered formulation to induce this lung-resident memory $CD8^+$ T cells can lead to a faster response upon infection and a better control of the viral infection in the lungs.

Finally, the study of the cell composition of the bronchoalveolar lavage (BAL) of immunized and infected mice showed an increased recruitment of T cells to the lungs in all vaccinated mice compared to control (Figure 6). Infected mice immunized subcutaneously showed a better recruitment of B cells while intranasal prime had an increased recruitment of $CD4^+$ T cells. Previous studies have shown that $CD4^+$ T cells can act synergistically with $CD8^+$ T cells to control influenza infections[42, 43], and perhaps contributed to the improved control of the infection in this group. Cationic liposomes have shown to be able to induce strong $CD4^+$ T cell responses as well as $CD8^+$ T cell responses[22]. Future research should study the delivery of both $CD8^+$ and $CD4^+$ T cell epitopes from influenza in cationic liposomes to induce a complete cellular immune response.

All in all, our work suggests that prime-boost vaccination strategies against respiratory viral infections could be more effective and powerful if the first immunization is administered intranasally.

CONCLUSION

Our study shows that intranasal immunization followed by a rapid systemic boost with a single-epitope liposomal subunit vaccine induces a potent $CD8^+$ T cell response both systemically and locally in the lungs. The local $CD8^+$ T cells elicited by vaccination expressed higher levels of CD103, associated to tissue-resident memory phenotype, and led to lower viral titers in lungs of influenza-infected mice compared to control.

AUTHOR CONTRIBUTIONS

FLV designed and carried out experiments, analysed the data, wrote the manuscript, and prepared the figures. DO performed experiments, analysed data, wrote and edited part of the manuscript. JAB and AK revised and edited the draft manuscript. BS and TCW conceptualised the project, provided input in the experimental design, revised, and edited the manuscript.

REFERENCES

1. Iuliano AD, Roguski KM, Chang HH, Muscatello DJ, Palekar R, Tempia S, et al. Estimates of global seasonal influenza-associated respiratory mortality: a modelling study. Lancet. 2018;391(10127):1285-300.
2. Pollard AJ, Bijker EM. A guide to vaccinology: from basic principles to new developments. Nat Rev Immunol. 2021;21(2):83-100.
3. Janssens Y, Joye J, Waerlop G, Clement F, Leroux-Roels G, Leroux-Roels I. The role of cell-mediated immunity against influenza and its implications for vaccine evaluation. Front Immunol. 2022;13:959379.
4. Sridhar S, Begom S, Bermingham A, Hoschler K, Adamson W, Carman W, et al. Cellular immune correlates of protection against symptomatic pandemic influenza. Nat Med. 2013;19(10):1305-12.
5. Rosendahl Huber S, van Beek J, de Jonge J, Luytjes W, van Baarle D. T cell responses to viral infections - opportunities for Peptide vaccination. Front Immunol. 2014;5:171.
6. Hu Y, Sneyd H, Dekant R, Wang J. Influenza A Virus Nucleoprotein: A Highly Conserved Multi-Functional Viral Protein as a Hot Antiviral Drug Target. Curr Top Med Chem. 2017;17(20):2271-85.
7. Mettelman RC, Allen EK, Thomas PG. Mucosal immune responses to infection and vaccination in the respiratory tract. Immunity. 2022;55(5):749-80.
8. Gould VMW, Francis JN, Anderson KJ, Georges B, Cope AV, Tregoning JS. Nasal IgA Provides Protection against Human Influenza Challenge in Volunteers with Low Serum Influenza Antibody Titre. Front Microbiol. 2017;8:900.
9. van Doremalen N, Lambe T, Spencer A, Belij-Rammerstorfer S, Purushotham JN, Port JR, et al. ChAdOx1 nCoV-19 vaccine prevents SARS-CoV-2 pneumonia in rhesus macaques. Nature. 2020;586(7830):578-82.
10. van Doremalen N, Purushotham JN, Schulz JE, Holbrook MG, Bushmaker T, Carmody A, et al. Intranasal ChAdOx1 nCoV-19/AZD1222 vaccination reduces viral shedding after SARS-CoV-2 D614G challenge in preclinical models. Sci Transl Med. 2021;13(607).
11. Burchill MA, Tamburini BA, Pennock ND, White JT, Kurche JS, Kedl RM. T cell vaccinology: exploring the known unknowns. Vaccine. 2013;31(2):297-305.
12. Rubin LG, Levin MJ, Ljungman P, Davies EG, Avery R, Tomblyn M, et al. 2013 IDSA clinical practice guideline for vaccination of the immunocompromised host. Clin Infect Dis. 2014;58(3):e44-100.
13. Nakamura T, Miyabe H, Hyodo M, Sato Y, Hayakawa Y, Harashima H. Liposomes loaded with a STING pathway ligand, cyclic di-GMP, enhance cancer immunotherapy against metastatic melanoma. J Control Release. 2015;216:149-57.
14. Karaolis DK, Means TK, Yang D, Takahashi M, Yoshimura T, Muraille E, et al. Bacterial c-di-GMP is an immunostimulatory molecule. J Immunol. 2007;178(4):2171-81.
15. Varypataki EM, Benne N, Bouwstra J, Jiskoot W, Ossendorp F. Efficient Eradication of Established Tumors in Mice with Cationic Liposome-Based Synthetic Long-Peptide Vaccines. Cancer Immunol Res. 2017;5(3):222-33.
16. Leal J, Smyth HDC, Ghosh D. Physicochemical properties of mucus and their impact on transmucosal drug delivery. Int J Pharm. 2017;532(1):555-72.

17. Varma DM, Batty CJ, Stiepel RT, Graham-Gurysh EG, Roque JA, 3rd, Pena ES, et al. Development of an Intranasal Gel for the Delivery of a Broadly Acting Subunit Influenza Vaccine. ACS Biomater Sci Eng. 2022;8(4):1573-82.

18. Slutter B, Pewe LL, Lauer P, Harty JT. Cutting edge: rapid boosting of cross-reactive memory CD8 T cells broadens the protective capacity of the Flumist vaccine. J Immunol. 2013;190(8):3854-8.

19. Pham NL, Pewe LL, Fleenor CJ, Langlois RA, Legge KL, Badovinac VP, Harty JT. Exploiting cross-priming to generate protective CD8 T-cell immunity rapidly. Proc Natl Acad Sci U S A. 2010;107(27):12198-203.

20. Budimir N, Meijerhof T, Wilschut J, Huckriede A, de Haan A. The role of membrane fusion activity of a whole inactivated influenza virus vaccine in (re)activation of influenza-specific cytotoxic T lymphocytes. Vaccine. 2010;28(52):8280-7.

21. Ahmed SF, Quadeer AA, McKay MR. Preliminary Identification of Potential Vaccine Targets for the COVID-19 Coronavirus (SARS-CoV-2) Based on SARS-CoV Immunological Studies. Viruses. 2020;12(3).

22. Benne N, van Duijn J, Lozano Vigario F, Leboux RJT, van Veelen P, Kuiper J, et al. Anionic 1,2-distearoyl-sn-glycero-3-phosphoglycerol (DSPG) liposomes induce antigen-specific regulatory T cells and prevent atherosclerosis in mice. J Control Release. 2018;291:135-46.

23. Badovinac VP, Messingham KA, Jabbari A, Haring JS, Harty JT. Accelerated CD8+ T-cell memory and prime-boost response after dendritic-cell vaccination. Nat Med. 2005;11(7):748-56.

24. Badovinac VP, Harty JT. Intracellular staining for TNF and IFN-gamma detects different frequencies of antigen-specific CD8(+) T cells. J Immunol Methods. 2000;238(1-2):107-17.

25. van Eenige R, Verhave PS, Koemans PJ, Tiebosch I, Rensen PCN, Kooijman S. RandoMice, a novel, user-friendly randomization tool in animal research. PLoS One. 2020;15(8):e0237096.

26. Belz GT, Xie W, Altman JD, Doherty PC. A previously unrecognized H-2D(b)-restricted peptide prominent in the primary influenza A virus-specific CD8(+) T-cell response is much less apparent following secondary challenge. J Virol. 2000;74(8):3486-93.

27. Townsend AR, Rothbard J, Gotch FM, Bahadur G, Wraith D, McMichael AJ. The epitopes of influenza nucleoprotein recognized by cytotoxic T lymphocytes can be defined with short synthetic peptides. Cell. 1986;44(6):959-68.

28. Anderson KG, Mayer-Barber K, Sung H, Beura L, James BR, Taylor JJ, et al. Intravascular staining for discrimination of vascular and tissue leukocytes. Nat Protoc. 2014;9(1):209-22.

29. Rotrosen E, Kupper TS. Assessing the generation of tissue resident memory T cells by vaccines. Nat Rev Immunol. 2023;23(10):655-65.

30. Slutter B, Van Braeckel-Budimir N, Abboud G, Varga SM, Salek-Ardakani S, Harty JT. Dynamics of influenza-induced lung-resident memory T cells underlie waning heterosubtypic immunity. Sci Immunol. 2017;2(7).

31. Chung C, Kudchodkar SB, Chung CN, Park YK, Xu Z, Pardi N, et al. Expanding the Reach of Monoclonal Antibodies: A Review of Synthetic Nucleic Acid Delivery in Immunotherapy. Antibodies (Basel). 2023;12(3).

32. Van Hoecke L, Job ER, Saelens X, Roose K. Bronchoalveolar Lavage of Murine Lungs to Analyze Inflammatory Cell Infiltration. J Vis Exp. 2017(123).

33. Naranbhai V, Nathan A, Kaseke C, Berrios C, Khatri A, Choi S, et al. T cell reactivity to the SARS-CoV-2 Omicron variant is preserved in most but not all individuals. Cell. 2022;185(6):1041-51 e6.

34. Koutsakos M, Illing PT, Nguyen THO, Mifsud NA, Crawford JC, Rizzetto S, et al. Human CD8(+) T cell cross-reactivity across influenza A, B and C viruses. Nat Immunol. 2019;20(5):613-25.

35. Gasper DJ, Neldner B, Plisch EH, Rustom H, Carrow E, Imai H, et al. Effective Respiratory CD8 T-Cell Immunity to Influenza Virus Induced by Intranasal Carbomer-Lecithin-Adjuvanted Non-replicating Vaccines. PLoS Pathog. 2016;12(12):e1006064.

36. Natalini A, Simonetti S, Favaretto G, Lucantonio L, Peruzzi G, Munoz-Ruiz M, et al. Improved memory CD8 T cell response to delayed vaccine boost is associated with a distinct molecular signature. Front Immunol. 2023;14:1043631.

37. Crowe SR, Turner SJ, Miller SC, Roberts AD, Rappolo RA, Doherty PC, et al. Differential antigen presentation regulates the changing patterns of CD8+ T cell immunodominance in primary and secondary influenza virus infections. J Exp Med. 2003;198(3):399-410.

38. Kallas EG, Grunenberg NA, Yu C, Manso B, Pantaleo G, Casapia M, et al. Antigenic competition in CD4(+) T cell responses in a randomized, multicenter, double-blind clinical HIV vaccine trial. Sci Transl Med. 2019;11(519).

39. Blobel NJ, Ramirez-Valdez A, Ishizuka AS, Lynn GM, Seder RA. Antigenic competition affects the magnitude and breadth of CD8 T cell immunity following immunization with a nanoparticle neoantigen cancer vaccine. The Journal of Immunology. 2017;198(1_Supplement):73.20-73.20.

40. Benne N. Vaccination and targeted therapy using liposomes : opportunities for treatment of atherosclerosis and cancer. The Netherlands: Leiden University; 2020.

41. Salomon R, Dahan R. Next Generation CD40 Agonistic Antibodies for Cancer Immunotherapy. Front Immunol. 2022;13:940674.

42. McKinstry KK, Strutt TM, Kuang Y, Brown DM, Sell S, Dutton RW, Swain SL. Memory CD4+ T cells protect against influenza through multiple synergizing mechanisms. J Clin Invest. 2012;122(8):2847-56.

43. Belz GT, Wodarz D, Diaz G, Nowak MA, Doherty PC. Compromised influenza virus-specific CD8(+)-T-cell memory in CD4(+)-T-cell-deficient mice. J Virol. 2002;76(23):12388-93.

SUPPLEMENTARY DATA

Supplementary Table 1. Details of SARS-CoV2-derived peptides loaded into cationic liposomes and used for in vivo screening. Binding affinity to HLA-A*11:01 predicted using NETMHCpan4.0

Peptide name	Amino acid sequence	Predicted binding affinity to HLA-A*11:01 (nM)	Protein	Protein accession number and position
COVN361	KTFPPTEPK	7.7	Nucleoprotein	P0DTC9 [361-369]
COVS1020	ASANLAATK	12.3	Spike	P0DTC2 [1020-1028]
COVN134	ATEGALNTPK	27.5	Nucleoprotein	P0DTC9 [134-143]
COVS757	GSFCTQLNR	44.4	Spike	P0DTC2 [757-765]
COVN310	SASAFFGMSR	30.9	Nucleoprotein	P0DTC9 [310-319]